Highlights

A new concept of water management diagnosis for a PEM fuel cell system

M. Ait Ziane, C. Join, M. Benne, C. Damour, N. Yousfi Steiner, M.C Pera

- Model-free fault detection approach is applied to PEMFC water management fault diagnosis.

- A theoretical proof is presented for model-free fault detection.

- Sensor fault is the main cause of water condensation and membrane dehydration.

- Real-time fault detection in the back pressure, temperature sensor and water management.

A new concept of water management diagnosis for a PEM fuel cell system

M. Ait Ziane[a,b], C. Join[c], M. Benne[a], C. Damour[a], N. Yousfi Steiner[b], M.C Pera[b]

[a]*ENERGY Lab, Univ.La Reunion, rue cassin, Saint-Denis, 97715, France*
[b]*FEMTO-ST, FCLAB, Univ. Franche-Comte,CNRS, rue Thierry-Mieg, Belfort, 90010, France*
[c]*CRAN,(CNRS,UMR 7039), Univ.Lorraine BP 239, Vandoeuvre-les-Nancy, 54506, France*

Abstract

This paper presents a new diagnosis view of fuel cell water management. The faults related to water management in the fuel cell are addressed from the control point of view and their occurrence is considered as a consequence of a temperature sensor fault. To ensure proper operation of the polymer electrolyte membrane fuel cell (PEMFC), the stack temperature and inlet pressure are controlled by a model-free control. A fault in the temperature sensor that causes an imbalance in water content in the stack is detected by a new fault detection approach in model-free context. The validation of the proposed strategy is performed on a 1.2 KW fuel cell with real time detection of temperature sensor faults, leading to water condensation in the cells or membrane dehydration. Fuel cell control and diagnosis are achieved without any requirement of an accurate system analytical model and additional sensors. However, faults can be detected in quasi static operation only and not un transient state.

Keywords: PEMFC water management diagnosis, Membrane dehydration, Water condensation, Sensor fault detection

1. Introduction

Greenhouse gas emissions reduction has become a worldwide major concern. Reducing dependence on fossil fuels and converting to green energy is one of the strategies adopted in recent years [1][2]. Among the technologies that have taken place in recent years in the green energy production chain is the Polymer Electrolyte Membrane Fuel Cell (PEMFC). The PEMFC system is an electrochemical converter [3] [4], that transforms air and hydrogen gases into electrical energy, heat and water with zero emission. These advantages have encouraged the utilization of this technology for a variety of stationary and mobile applications [5].

The combination of a variety of phenomena (electrical, fluidic, thermal) is making the PEM fuel cell a rather complex system [6]. This complexity has a direct effect on system durability, which hinders large-scale commercialization. In operation, water management is considered a crucial key to solve this problem, as the PEMFC constantly produces water and is extremely sensitive to the water balance. Excess liquid water inside the cells can slow down the electrochemical reaction and reduce PEMFC performance[7]. Massive water droplet formation in the flow channel or inside the electrodes leads to a flooding fault [8]. In the opposite case when the membrane is poorly hydrated, the drying fault can appear. Flooding may be induced by various factors which can occur simultaneously, such as a reduced fuel cell temperature, elevated inlet gas humidity [9], and reduced gas flow [10]. The opposite operating conditions lead to the membrane to dry out [10]. For this purpose, controlling the temperature and relative humidity is mandatory to maintain membrane water balance and to minimize the potential of these faults occurrence [11]. Poor gas control can lead to starvation fault when there is insufficient flow to sustain the required current. In case of overflow, the water can be drained out of the membrane and lead to drying out [12]. Membrane degradation can be caused by a large difference in inlet pressure between the electrodes. Consequently, a rigorous control of the inlet pressure is necessary [13]. Unless these faults are remedied immediately, the fuel cell may be damaged beyond recovering. To this end, proper control of these operating conditions and early detection of these faults are crucial to improve PEM fuel cell lifespan.

More generally, the fault can be considered as a change in the state of the system that prevents it from completing the assigned task [14]. Commonly, the faults can be classified into actuator, sensor and system faults [15]. In recent years, significant work has focused on fault detection and diagnosis (FDD) in order to prevent system damage [16]. The most common approach used for fault diagnosis is model-based. The concept consists in designing a model that faithfully represents the system real behavior in order to verify its consistency with the actual one [17]. Generally, the system's measured output is checked against the one obtained from the model by evaluating a residual signal. This latter is seen as a fault indicator in case of residual discrepancy [18]. Observers are widely used for system diagnosis, estimating outputs or the internal state of the system that cannot be measured [19] [20]. The model based approach has proven a good efficiency in systems fault diagnosis. However, the most critical step is obtaining an accurate model representing the real behavior of the system. Increasingly, the systems architecture is growing more complex, making this task challenging. To face this difficulty, the non-model based approach is suitable for diagnosing complex systems where the precise physical model is unknown.

Several methods are regarded as a non-model based: fault detection based signal [21] [22], statistical [23] and Artificial Intelligence [24]. Signal-based methods use the measured signal from the system to detect faults symptoms. Statistical methods are supported by data analysis to deal with uncertainties and system noise as well as to assess the probability that the system state is faulty. These methods are widely used for manufacturing systems. Artificial intelligence methods are also widely used owing to their ability to analyze and classify data to detect failures even with very low level of knowledge of the system. [25].

Basically, proper control of the PEM fuel cell operating parameters ensures smooth operation and can avoid these malfunctions. However, the controller effectiveness is disturbed by faults, as faults impact the main components of the control loop. As mentioned before, faults are classified into three types:

- Fault on the actuator that affects its performance by degrading its ability to operate.

- Fault on the sensor that leads to sending erroneous measurements.

- Fault on the system that impacts its operation, and may take it out of the nominal operating range.

For some complex systems such as the PEM fuel cell, a fault on an actuator or a sensor can lead to a system fault [26]. Therefore, an appropriate diagnosis tool able to detect all these faults is required to achieve a more sustainable PEM fuel cell.

This paper proposes to study the significant link between the control and the diagnosis of the PEMFC operating conditions. To our knowledge, the topic of PEMFC water management diagnosis has never been addressed as integrated in the controller development. As mentioned before, an appropriate control ensures the proper functioning of the PEMFC, of course, but in some cases it is not enough. For this reason, diagnosis of the whole system is essential in order to assess its operating condition. To ensure proper operation of the PEM fuel cell, the control of the stack temperature and inlet pressure is addressed. Regarding the diagnosis part, the association between a fault on the temperature sensor and its effect on faults appearance related to water management is highlighted. The water management faults investigated are water condensation in the cells and membrane dehydration, which are considered as system faults. The following section presents the different methods and aspects handled in the framework of fuel cell water management fault diagnosis.

To provide proper control of the operating conditions of the PEMFC, a model-free controller (MFC) [27] is employed to regulate the stack pressure and temperature. The controller is mainly driven by an ultra-local model instead of the entire analytical model of the system. A model-free fault detection (MFFD) approach inspired by the controller is presented and applied in real time for fault detection of actuators, sensors and related water management faults. The method is mainly based on the estimation of the ultra-local model output which is considered in the control part. The obtained estimated output is corrected by a parameter in order to obtain a zero residual signal in the absence of a fault. The authors of [50] [51] have briefly presented the method without being exhaustive on details and without justifying the introduction of such a parameter for the correction of the estimated output. Furthermore, the method is applied to academic examples through simulations in order to detect only actuator faults. In this paper, a real-time application is performed on a 1.2 kW fuel cell to detect actuator, sensor and system faults. A theoretical proof is given regarding the parameter used in the correction of the estimated output. This proof emphasizes the conditions under which faults can be detected. This means that the limitations and merits of the proposed method are well illustrated both theoretically and by real-time experimental validation. Furthermore, the diagnosis of the PEMFC is presented by establishing a link between the control of its operating conditions and the occurrence of water management related faults.

The structure of the paper is as follows: a review of the current literature on water management diagnosis methods is provided in the second section. In the third section, a presentation of model-free controller (MFC) and model-free fault detection (MFFD) is provided. The fourth section discusses the control of the operating conditions of the stack. Experimental validation dealing with sensor, water management faults detection is presented in fifth section. Conclusion and perspective are given in the sixth section.

2. Diagnosis methods

Basically, most of the approaches and methods presented above are applied to PEMFC water management diagnosis. A model-based method providing an estimation of the liquid saturation in the cathode side and the current density is presented in [28]. Current density estimation is considered as an index to detect flooding and starvation faults. An unscented Kalman Filter is applied on the simplified model of PEM fuel cell under simulation environment in [29]. Cell voltage, current, and inlet pressure are set as inputs to a Kalman filter, which is used to diagnose a fault. Flooding is detected by estimating the quantity of water in both anode and cathode

channels. To estimate the membrane conductivity, the authors of [30] use a sliding mode observer. The conductivity of the membrane is expressed as a relation to the water concentration, allowing detection of the flooding and drying state. For the same purpose of estimation, an extended Luenberger observer is applied in [31].

As a matter of fact, the production of water takes place at the cathode. Excessive water will first accumulate in the electrode or in the cathode channels. Water droplet accumulation across the flow channels and the gas diffusion layer leads to an increase in cathode pressure drop [32] [33]. Therefore, cathode pressure drop can be taken as an appropriate indication of flooding occurrence [34] [35]. So, there are several works in the literature that rely on cathodic pressure drop for flooding and drying detection [36] [37] [38]. Authors in [39] compare the theoretical pressure drop with the measured value to determine the flooding. Once the measured pressure drop exceeds the calculated one, a flooding is detected. A neural network model is employed in [40] to detect flooding and drying which are supposed to be the only faulty cases possible. The validation of the model is performed offline with normal fuel cell operation data. Two residuals are generated to assess the coherence of the collected voltage and the cathode pressure drop with those obtained by the neural network under normal operating conditions. Water condensation fault is detected when the two residues diverge from zero. On the contrary, cathodic pressure drop is unaffected by membrane drying. Only the stack voltage drops, which entails a divergence on the voltage residual, thus isolating the fault.

Most of the model-based approaches mentioned above are validated by a simulation. Experimental test and real-time validation is a challenging task due to the difficulty of obtaining a model that perfectly describes the PEMFC system. Signal-based methods are commonly adopted for water management fuel cell diagnosis. A combination of Wavelet Transform and an entropy feature extraction is applied experimentally in [41]. Only the voltage signal is used for the detection and isolation of four types of faults. Experimental results revealed that high and low oxygen stoichiometry, cooling rate, flooding, drying and fuel cell poisoning faults have a direct impact on entropy and can be easily detected and isolated. A Wavelet Transform is applied on the 40-cell stack to detect the high stoichiometry fault that can lead to membrane drying in [42]. The signals considered for the diagnosis are: stack voltage, individual cell voltage and the air pressure drop. Fault detection is accomplished on the basis of the energy present in each wavelet decomposition detail. A Fast Fourier Transform is applied on 5-cell stack [43].
Statistical methods are also employed for PEMFC fault diagnosis. Based on the

collected cell voltage data, cathode and anode pressure drop signals, a diagnostic strategy is carried out in [44]. The considered method is related to the calculation of statistical descriptor level of cell voltage which is susceptible to water management. A statistical descriptor of pressure fluctuation is also calculated to identify flooding and drying faults. In addition, artificial intelligence is being introduced on a large scale for the diagnosis of water management. A binary encoding convolutional neural network is applied on 120 KW PEM fuel cell stack in [45]. The results revealed that flooding, drying and starvation faults are detected and isolated by specifying their severity. A fuzzy neural approach relying on electrochemical impedance spectroscopy is presented in [46]. An equivalent circuit model identification is performed for anode and cathode impedance. Based on the obtained equivalent circuit model, neural fuzzy inference is used to detect flooding and drying faults.

This non-exhaustive bibliography deals, in particular, with PEMFC water management diagnosis resulting in flooding and drying faults. Implementing these methods for real time diagnosis is an arduous task, hence the validation of most of these approaches is performed offline with experimental data.

Whatever the strengths and weaknesses of the application of these methods, the problem that should be addressed is how these faults are generated during the measurement campaign. In most cases, flooding and drying are induced by a voluntary change in PEMFC operating conditions. The main changes in the operating condition variables are as follows: stack temperature [47] [45] [41][46] [48], relative humidity [45] [44] [40] [43] and gas stoichiometry [42][46]. It is widely demonstrated that these alterations lead to the occurrence of flooding and membrane drying faults [49]. In our opinion, the relevance of applying a diagnostic tool when the fault is generated by an intentional change in the operating conditions is disputable. Indeed, when these parameters are controlled in a closed loop in the presence of a controller that is robust to disturbances, the temperature, relative humidity, and gas flow are maintained at their desired operating condition and never change. Therefore, with a robust controller taking into account the fuel cell dynamics and ageing, there is no reason to provoke a water management fault. This might be valid unless there is a fault affecting the components of the control loop (actuator, sensor). In this case, it is important to detect the origin of the fault, which can be an actuator fault preventing the PEMFC cooling or a sensor fault that can send wrong information and its consequences on the system, which can lead to the initiation of water condensation in the stack and membrane dehydration faults. Therefore, the issue of water management related faults is addressed in this paper as a consequence of one or more

failures occurring upstream and resulting in a change in operating parameters that lead to a system fault.

The major contribution of the present study is to highlight that even with an appropriate control of these parameters, a fault on the temperature sensor can be at the origin of water management faults occurrence. In this context, the first considered action is to properly control the stack temperature and input pressure difference between the electrodes. Controlling inlet pressure drop prevents membrane degradation. Secondly, the temperature sensor fault is considered to emphasize its effect on the occurrence of imbalance in the water content of the PEMFC.

A model-free controller or $(iPID)$ [27] is employed to control the operating conditions of the stack. An ultra-local model, updated at each time point, is used instead of the global fuel cell model for the controller design. The uncertain part of the system is estimated online only with the latest input and output measurements. Additionally, major advantages of the proposed approach for real-time applications are the low computation cost and the simplicity of implementation.

Regarding the diagnosis part, a new model-free fault detection approach, which is regarded as an expansion of the controller, is introduced in this paper. The authors of [50] have applied the proposed method on academic examples in simulation to detect an actuator fault. In this paper, a theoretical proof is presented to explain in detail the limitations and the performance of the model-free fault detection approach. A real-time experimental validation for the detection of faults that affect the back pressure valve, temperature sensor, flooding and drying faults are discussed in the present paper. The method is mainly driven by the estimation of the ultra-local model output which is considered in the control part. A residual signal, qualified as a fault presence indicator, is obtained from the comparison of the estimated and the measured output. The intention is to emphasize that in a real application the flooding and drying faults that are considered as system faults can be studied as a consequence of a fault on the sensor that measures the stack temperature.

3. Control and diagnosis in a model-free context

The presented approach is mainly driven by the model-free controller $(iPID)$ [52] [27] which has proven to be very efficient for controlling nonlinear systems [53] [54]. Moreover, it can both reject disturbances and tolerate faults affecting the system. The principal of model-free control, i.e. without an analytical model, is briefly summarized below.

The basis of $iPID$ is to substitute the overall system physical model by an ultra-local model. The latter is described in this way:

$$y^{(\nu)} = F + \alpha.u \tag{1}$$

Where:

- y represents system measured output and u is system input.

- (ν) refers to the derivation order of y.

- α is a constant chosen by the user.

- The unknown part of the system is included in the function F.

An algebraic estimation approach is presented in [55] [56] [57] to estimate the function F. For a first-order ultra-local model, i.e. $\nu = 1$, this function can be estimated as:

$$\hat{F}(t) = \frac{-3!}{L^3} \int_{t-L}^{t} (y(\sigma)(L - 2\sigma) + (L - \sigma)\alpha\sigma u(\sigma)) \, d\sigma \tag{2}$$

The integration range $[t - L; t]$ is referred to the sliding window, $L > 0$ being considered small. The iP control law is defined by :

$$u(t) = \frac{1}{\alpha} \left(-\hat{F}(t) + \dot{y}_d(t) + k_p e(t) \right) \tag{3}$$

The estimate of F for $\nu = 2$ is defined by :

$$\hat{F}(t) = \frac{5!}{L^5} \int_{t-L}^{t} \left(L^2 + 6\sigma^2 - 6L\sigma \right) y(\sigma) d\sigma - \left(\frac{\alpha\sigma^2}{2}(L^2 + \sigma^2 - 2L\sigma)u(\sigma) \right) d\sigma \tag{4}$$

The iPD controller can be employed in the case of $\nu = 2$, the input u is calculated as follows:

$$u(t) = \frac{1}{\alpha} \left(-\hat{F} + \ddot{y}_d + k_p e + k_d \dot{e} \right) \tag{5}$$

Where :

- y_d and $\dot{y}_d$ the desired trajectory and its derivative respectively.

- $e = y_d - y$ the trajectory tracking error and $\dot{e}$ its derivative.

- k_p and k_d controller gains.

More illustrations about the method are presented in [58] [59].

3.1. Model-free fault detection:

In this approach, the focus is on generating a residual signal. The residual is achieved through measuring and estimating the measured system output. From Eq.1, the system output can be estimated.

Considering $\nu = 1$, from Eq.1 the output y can be described as below:

$$y(t) = \int_0^t \left(F(\sigma) + \alpha u(\sigma) \right) d\sigma + y(0) \tag{6}$$

The estimate of F is imprecise due to various factors, is expressed by:

$$\Delta F(t) = F(t) - \hat{F}(t) \tag{7}$$

Replacing Eq.7 in Eq.6 yields to:

$$y(t) = \int_0^t \left(\hat{F}(\sigma) + \alpha u(\sigma) + \Delta F(\sigma) \right) d\sigma + y(0) \tag{8}$$

Theoretically, the estimated output $\hat{y}$ can be obtained by:

$$\hat{y}(t) = \int_0^t \left(\hat{F}(\sigma) + \alpha u(\sigma) \right) d\sigma + \hat{y}(0) \tag{9}$$

Under a null estimation error assumption, $\Delta F(t) = 0$, then $\hat{y}(t) = y(t)$, although there is a fault, it is not detectable. However, $\Delta F(t) \neq 0$, $\hat{y}(t) \neq y(t)$ in the convenient case. For this purpose, a correction of $\hat{y}(t)$ is performed with the parameter β. More details on the evolution of β is presented in [50]. In what follows, an illustration on the significance of β parameter in the correction of $\hat{y}$ and the condition in which the actuator and sensor faults can be detected with the proposed method.

Proposition 1. *The residual employed for fault detection may be described in the following way:*

$$r(t) = y(t) - \beta \hat{y}(t) \tag{10}$$

The retained β is the value of $\beta(t)$ in normal operation, this latter is expressed as:

$$\beta(t) = \frac{y(t)}{\hat{y}(t)} = \frac{y(t)}{\int_0^t \left(\hat{F}(\sigma) + \alpha u(\sigma) \right) d\sigma + \hat{y}(0)} \tag{11}$$

The initial condition $\hat{y}(0)$ is considered known and should be taken as $\hat{y}(0) \simeq y(0)$.

To simplify the study, the following demonstration on β is performed in discrete form and the output is assumed to be noise free. The tools that can be used for the discretization procedure are defined thereafter.

In the absence of noise, the derivative of a function can be obtained by finite difference as follows:

$$\frac{dS(t)}{dt} \simeq \hat{\dot{S}}(k) = \frac{S(k) - S(k-1)}{T_e} \tag{12}$$

Where T_e is the sampling period. The method of rectangles which is denoted by $\mathcal{I}$ can approximate a time integral, where :

$$\int_0^t S(\tau)d(\tau) \simeq \mathcal{I}(S(k)) = \sum_{i=1}^k S(i).T_e \tag{13}$$

Proof. To demonstrate that β is converging to a constant value in the absence of a fault for any change of setpoint for all linear and some nonlinear systems in the case of $\nu = 1$, this procedure is followed:

From Eq.1, $\hat{F}$ can be written as such:

$$\hat{F}(k) = \hat{\dot{y}}(k) - \alpha u(k-1) \tag{14}$$

The estimated function $\hat{F}$ cannot use $u(k)$ due to causality. Applying the finite difference expressed by Eq.12 for the output y, this gives:

$$\hat{\dot{y}}(k) = \frac{y(k) - y(k-1)}{T_e} \tag{15}$$

From Eq.13. and Eq.9, $\hat{y}(k)$ can be represented in discrete form by:

$$\hat{y}(k) = \mathcal{I}\left(\hat{F}(k) + \alpha u(k)\right) + \hat{y}(0) \tag{16}$$

By replacing Eq.14 into Eq.16, it yields:

$$\hat{y}(k) = \mathcal{I}\left(\hat{\dot{y}}(k) - \alpha u(k-1) + \alpha u(k)\right) + \hat{y}(0) \tag{17}$$

Using the finite difference integral defined by Eq.13 in Eq.17, this gives:

$$\mathcal{I}(\hat{\dot{y}}(k)) = \mathcal{I}(\frac{y(k) - y(k-1)}{T_e}) = \frac{y(1) - y(0)}{T_e} \times T_e +$$
$$\frac{y(2) - y(1)}{T_e} \times T_e + ... + \frac{y(k) - y(k-1)}{T_e} \times T_e = y(k) - y(0) \tag{18}$$

$$\mathcal{I}(\alpha u(k) - \alpha u(k-1)) = \alpha.T_e.(u(k) - u(0)) \tag{19}$$

In the control law synthesis, the initial condition $u(0) = 0$, this gives :

$$\hat{y}(k) = y(k) - y(0) + \hat{y}(0) + \alpha T_e.u(k) \tag{20}$$

The iP controller ensures the stability of the controlled systems, which means that a steady state can be achieved. In fault free case, in steady state we get:

$$u(k) = c(k).y(k) \tag{21}$$

$c(k)$ denotes a parameter assigned to the controlled system. Substituting Eq.21 in Eq.20, it gives:

$$\hat{y}(k) = y(k)\,(1 + T_e.\alpha.c(k)) - y(0) + \hat{y}(0) \tag{22}$$

Substituting Eq.22 into Eq.11, $\beta(k)$ can be expressed as follows:

$$\beta(k) = \frac{y(k)}{\hat{y}(k)} = \frac{y(k)}{y(k)\,(1 + T_e.\alpha.c(k)) - y(0) + \hat{y}(0)} \tag{23}$$

$\hat{y}(0)$ is considered known and must be taken equal to $y(0)$, this leads to:

$$\beta(k) = \frac{y(k)}{\hat{y}(k)} = \frac{y(k)}{y(k)\,(1 + T_e.\alpha.c(k))} = \frac{1}{1 + \alpha.c(k).T_e} \tag{24}$$

It is then straightforward that if $c(k)$ is constant then β is always constant too. This property applies to all systems, linear or nonlinear, having a linear static characteristic, which gives:

$$\beta = \frac{y(k)}{\hat{y}(k)} = \frac{1}{1 + \alpha.c.T_e} \tag{25}$$

Eq.25 proves that β always converges to a constant value for any established steady-state, that means for any variation of the trajectory in the absence of a fault.
In fault-free case, β is constant and $r(t) = 0$. In the case of an actuator fault and disturbance, the static characteristic of the controlled system represented by Eq.21, changes and becomes:

$$u_f(k) \neq c(k).y(k) \tag{26}$$

In the presence of sensor fault Eq.21 become:

$$u(k) \neq c(k).y_f(k) \tag{27}$$

11

Where u_f refers to the calculated input to tolerate a fault, and y_f to the measured output which does not represent system state.

The residual r is never zero $y \neq \beta \hat{y}$ once the system static characteristic is changed, which enables fault detection. $\qquad\square$

For a real time application and for systems that do not have a linear static characteristic, β needs to be readjusted for every change of set point, it is proposed to adapt it as bellow:

Algorithm 1 β adaptation

1: $\beta(0) = 1$
2: **if** $\dot{y}_d(t) = 0$ and $e(t) \approx 0$ **then**
3: $\quad \beta \leftarrow \beta(t-1)$
4: **else**
5: $\quad \beta(t) \leftarrow \frac{y(t)}{\hat{y}(t)}$
6: **end if**

It should be mentioned that faults cannot be detected in the transient state for systems that do not have a linear static characteristic. Where $e = y_d - y$ and $e \approx 0$ means that the steady state is reached, so the last calculated value of β is retained for that operating point. Note that the initial condition of the estimated output should be taken as the measured condition.

3.2. Control and diagnosis objective

The two PEMFC operating conditions that are considered for the control are: stack temperature and inlet pressure. Membrane degradation can be avoided by keeping the inlet pressure at the same level. Fault detection is addressed at two levels. The first level deals with faults that impact the control loop such as the actuator and sensor. Regarding actuator fault, a power loss is introduced to the valve that controls the stack pressure. This fault is addressed as an illustration of the presented model-free fault detection approach. In the case of sensor fault, an offset is induced on the temperature sensor. The consequences of this fault on the PEM fuel cell, leading to water management fault are studied as a second level of fault detection. The detection and isolation of water condensation in the cells and membrane dehydration are also achieved.

4. Pressure and temperature control

4.1. Fuel cell test bench

The experimental rig used for all tests is conceived for PEM fuel cells with a nominal power of 1.5 KW. Mass flow measurement and control is provided by two mass flow controllers for each sides. The relative humidity of the inlet gases is monitored through adjusting boiler temperature and inlet gas heat. The inlet and outlet pressure is measured by sensors for both sides. The stack pressure is managed thanks to back pressure valves. Stack temperature is controlled through three elements: the pump that controls the cooling flow rate of primary circuit, an electro-valve that controls the flow of water through the exchanger to cool the primary circuit and a heater that heats-up the water at the start of the test. The control and acquisition of data is performed using LabView under NI PXI-1031 with a sampling frequency of 3Hz. The proposed control and diagnosis strategy are implemented in real-time. All experiments are performed on a 1.2 KW nominal power stack composed with 12 cells having an active surface of 90 cm^2.

4.2. Pressure control and back pressure fault detection

As previously mentioned, controlling the inlet pressure prevents membrane mechanical degradation, which can lead to irreversible damage. For the studied stack, the manufacturer recommends not to exceed 300 mbar. Fig.1 illustrates the control and diagnosis approach adopted. For the hydrogen inlet pressure, a second-order ultra-local model is employed, which results in iPD. For the air inlet pressure, a first-order ultra-local model is selected, corresponding to a iP controller. Note, that there is no specific rule for choosing the ultra-local model order when designing the system input. Usually, a first-order, i.e (iP) is used first. If the result is unsatisfactory, a second-order model is required.

The actuator fault is triggered by the decrease in air pressure feeding the back pressure valve. The recommended pressure for this device is 2 bar, which is regarded as a normal condition for the proper operation for this component. A decrease in the pressure of the air supplying the back pressure valve of about 1 bar induces the fault. In fact, this fault entails a performance loss of the back pressure valve. In an actual system, it can occur as a result of a leak in the air supply circuit.
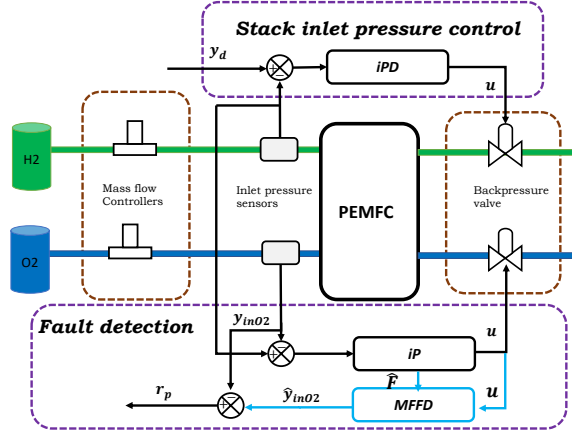
Figure 1: Control and fault detection strategy

The second-order ultra-local model employed for the anode side is represented by:

$$\ddot{y}_{inH2} = F_{inH2} + \alpha_1 . u_{inH2} \tag{28}$$

Where the input is taken as:

$$u_{inH2} = \frac{1}{10} \left(-\hat{F}_{inH2} - 3e - 30\dot{e} + \ddot{y}_d \right) \tag{29}$$

where $e = y_d - y_{inH2}$ and $\dot{e}$ its derivative. y_d is the desired inlet pressure for both sides.

Concerning the cathode inlet pressure, the first order ultra-local model employed is given as follows:

$$\dot{y}_{inO2} = F_{inO2} + \alpha_2 . u_{inO2} \tag{30}$$

The input is given as follows:

$$u_{inO2} = \frac{1}{0.3} \left(-\hat{F}_{inO2} + 0.1e + \dot{y}_{inH2} \right) \tag{31}$$

where $e = y_{inH2} - y_{inO2}$. The parameters of the iP and $iPID$ controllers are determined empirically, i.e. with a trial and error method. The estimation of the inlet pressure cathode is calculated as follows:

$$\hat{y}_{inO2}(t) = \int_0^t \left(\hat{F}_{inO2}(\sigma) + 0.3 . u_{inO2}(\sigma) \right) d\sigma + y_{inO2}(0) \tag{32}$$

The estimated inlet air pressure should be corrected by β_p to achieve a zero residual when there is no fault. Since the PEMFC is a strongly nonlinear system, this

parameter evolves with changes in set point. The residue is written in the following form:

$$r_p(t) = y_{inO2}(t) - \beta_p \hat{y}_{inO2}(t) \tag{33}$$

Where β_p corresponds to $\beta_p(t)$ in permanent state, obtained by the **Algorithm1**.

The entire experiment lasts 60min, the initial 25min are spent varying the desired trajectory to ensure that the controller guarantees a minimum inlet pressure difference between the electrodes. The objective is also to analyze the evolution of β_p for different set point changes. The actuator fault is triggered in the interval [32min-51min]. Fig.2(a) shows the overall experimental test for inlet pressure difference and fault detection on the back pressure valve. Both controllers iPD and iP provide an excellent trajectory tracking as shown in Fig.2(b). For all desired trajectory changes, the maximum inlet pressure difference is about 25 mbar. This is well below the maximum required level as seen in Fig.2(c). This confirms that the proposed control strategy preserves the fuel cell stack from mechanical damage. Increasing the inlet pressure enables to enhance the performance and the power delivered by the stack, as shown in Fig.2(d). This confirms the fact that proper stack pressure control contributes to achieve the best PEMFC performance.

Additionally, the estimated inlet cathode pressure follows perfectly the measured one in fault free case, for all changes of desired trajectory 2(b). The evolution of the parameter β is shown in Fig.2(e), for each change of desired trajectory this latter is recalculated. The calculation of this parameter is performed with Algorithm 1. When the set point changes, this parameter is varying and is expressed by $\beta_p(t) = \frac{y_{inO2}(t)}{\hat{y}_{inO2}(t)}$, for which the noise is present in Fig. 2(e). Once the output stabilizes around the setpoint, i.e. $(e \approx 0)$, the last calculated value of $\beta_p(t-1)$ is retained until the next setpoint change. The stack inlet pressure is established at 1750 mbar from 24th minute. The estimated inlet cathode pressure corresponds to the measured up to the time of fault occurrence at 32nd minute.

The fault is triggered with 1 bar pressure drop in the air pressure supplying the back pressure valve. A divergence is immediately noticed on the estimated inlet pressure, Fig.2(f). The cathode inlet pressure is impacted also by this fault and drops to 1740 mbar. Since the iP controller is tolerant of actuator fault, the cathode inlet pressure is quickly restored to the set point. The occurrence of the fault has an impact on the voltage signal which undergoes a fluctuation. The residual signal remains around 0 bar for all setpoint changes until the fault occurs and then diverges to -25 as shown in Fig.2(g). This allows the fast detection of backpressure actuator fault. The residual signal returns at the initial position once the fault disappears at 51st minute.

It should be noted that the applied control strategy tolerates the fault by ensuring a pressure difference around 0 even in case of a fault. On top of that, the model-free fault detection method allows the fast and real-time detection of the fault without any additional equipment. These facts are considered to be the main advantage of the proposed strategy.
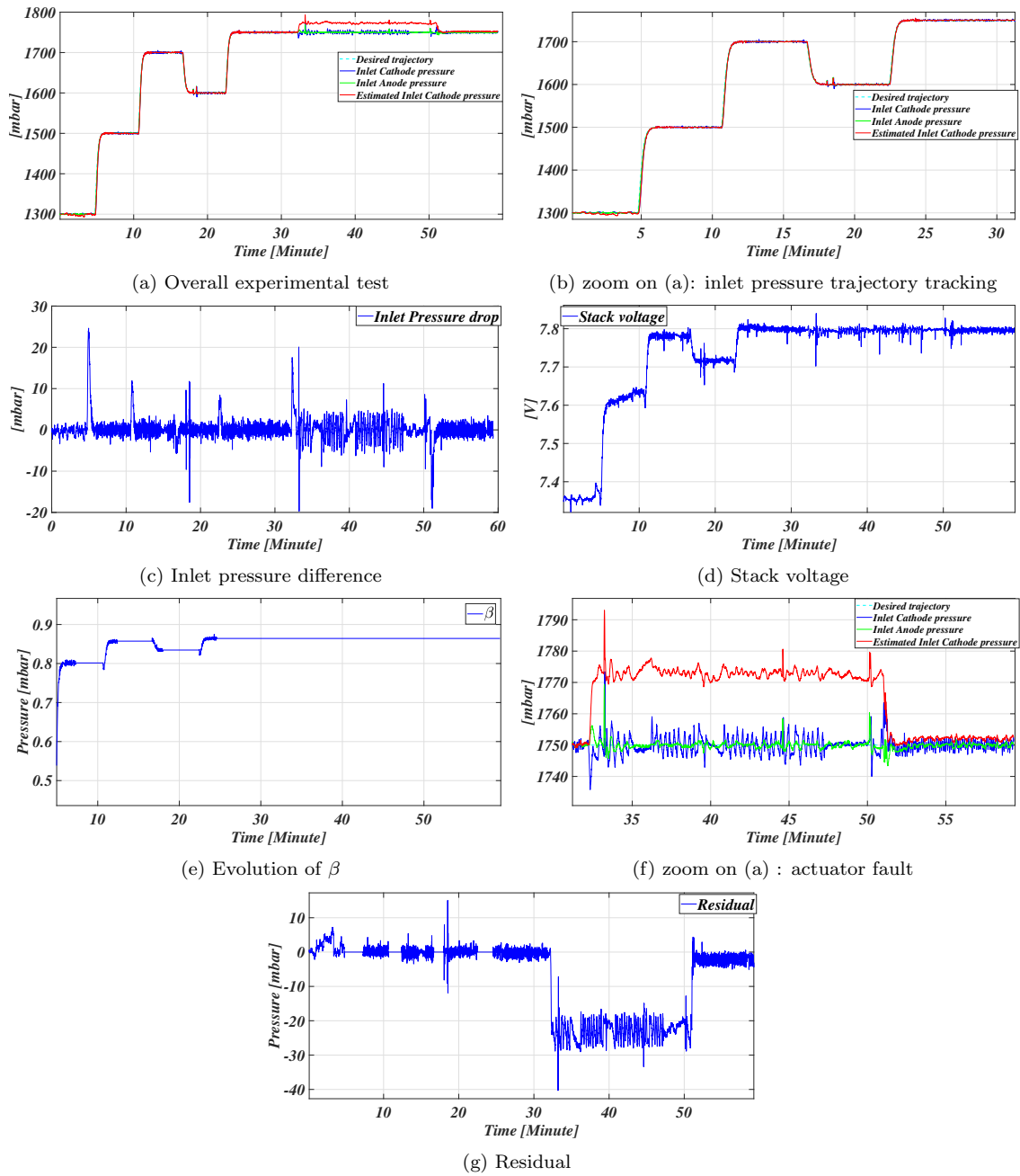
(a) Overall experimental test

(b) zoom on (a): inlet pressure trajectory tracking

(c) Inlet pressure difference

(d) Stack voltage

(e) Evolution of β

(f) zoom on (a) : actuator fault

(g) Residual

Figure 2: Actuator fault detection

4.3. Temperature control

The temperature control strategy is achieved by controlling the flow of cooling water through the exchanger, water primary circuit flow and the heating resistor. The primary circuit flow is controlled by an iP controller. The manipulated variable is pump speed. The stack temperature control strategy is achieved by acting on the flow rate of the secondary circuit of the exchanger and the heater at the beginning of the test. The global scheme of the temperature control is presented in Fig.3.

The architecture of the overall control strategy is cascading ensured by two iP controllers. The first one is employed to compare the desired temperature with the measured one at stack output to generate an inlet temperature reference. This reference is regulated with respect to the inlet fuel cell cooling temperature, which is provided by the second iP controller. The cooling water flow rate is also regulated by an iP controller but separately, i.e. it is regulated according to the desired flow rate and is independent from the stack temperature.
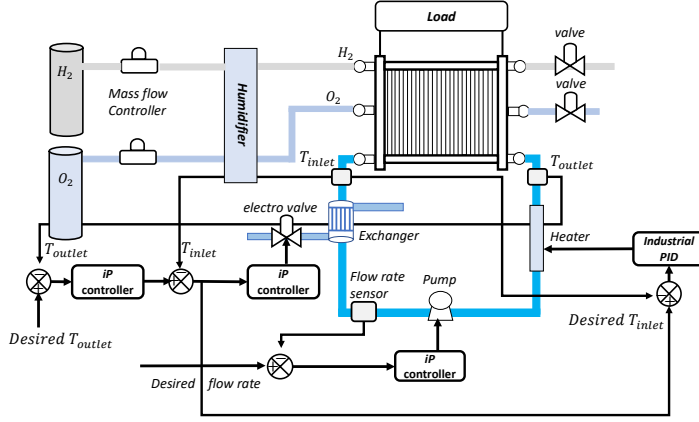

Figure 3: Temperature management and sensor fault detection

Three first order ultra-local model are employed to perform the temperature control strategy. The first one, is related to the global strategy that is given as:

$$\dot{y}_{Tout} = F_{Tout} + \alpha_3.u_{Tout} \tag{34}$$

The input is given as follows:

$$u_{Tout} = \frac{1}{30}\left(-\hat{F}_{Tout} + 0.5e + \dot{y}_{dTout}\right) \tag{35}$$

Where: $e = y_{dTout} - y_{Tout}$. y_{dTout} is the desired temperature of stack and y_{Tout} is the measured stack temperature.

The estimated outlet stack temperature is calculated by:

$$\hat{y}_{Tout}(t) = \int_0^t \left(\hat{F}_{Tout}(\sigma) + 30.u_{Tout}(\sigma) \right) d\sigma + y_{Tout}(0) \tag{36}$$

For the control of the inlet temperature, a first-order ultra-local model is employed, and is expressed as follows:

$$\dot{y}_{Tin} = F_{Tin} + \alpha_4.u_{Tin} \tag{37}$$

The input can be expressed as follows:

$$u_{Tin} = \frac{1}{10} \left(-\hat{F}_{Tin} - 10e + \dot{y}_{dTin} \right) \tag{38}$$

Where: $e = y_{dTin} - y_{Tin}$, y_{Tin} is the measured inlet temperature of the PEMFC and $y_{dTin} = u_{Tout}$.
The ultra-local model for primary water circuit flow is given as:

$$\dot{y}_{Cool} = F_{Cool} + \alpha_c.u_{Cool} \tag{39}$$

The input is given as:

$$u_{Cool} = \frac{1}{3} \left(-\hat{F}_{Cool} + 1.5e + \dot{y}_{dCool} \right) \tag{40}$$

Where: $e = y_{dCool} - y_{Cool}$, y_{dCool} is the desired cooling rate and y_{Cool} is the measured one.

The operating temperature recommended by the PEMFC manufacturer is between 70°C and 75°C. The outlet fuel cell cooling temperature is controlled at 72°C. The control's objective is to keep stack temperature at the desired value for each current change. High load demands result in additional heat generation by the PEM fuel cell. An effective control strategy maintains better performance, dissipates this heat and ensures a better water balance inside the cells.

The validation of the control strategy is done under a steps of current in [18A - 105A], Fig.4(a). These current variations are considered as disturbances for the control strategy. The outlet stack cooling temperature is maintained around the desired temperature with peaks of ±2 degrees for the large current demand as illustrated in Fig.4(b). These fluctuations would also occur during actual operation of PEMFC systems submitted to large current variations. The stack temperature is adjusted at the required operating condition 72°C after one minute of current variation. In such cases, the controller ensures that the temperature of the PEMFC is properly

19

controlled, whatever the load changes. Stack voltage signal is presented in Fig.4(c). It can be observed that after each current change, stack voltage stabilizes at a value corresponding to the new level of current and remains constant. No additional voltage drop is observed, which signifies that the stack is operating under normal conditions.

(a) Current profile

(b) Stack temperature
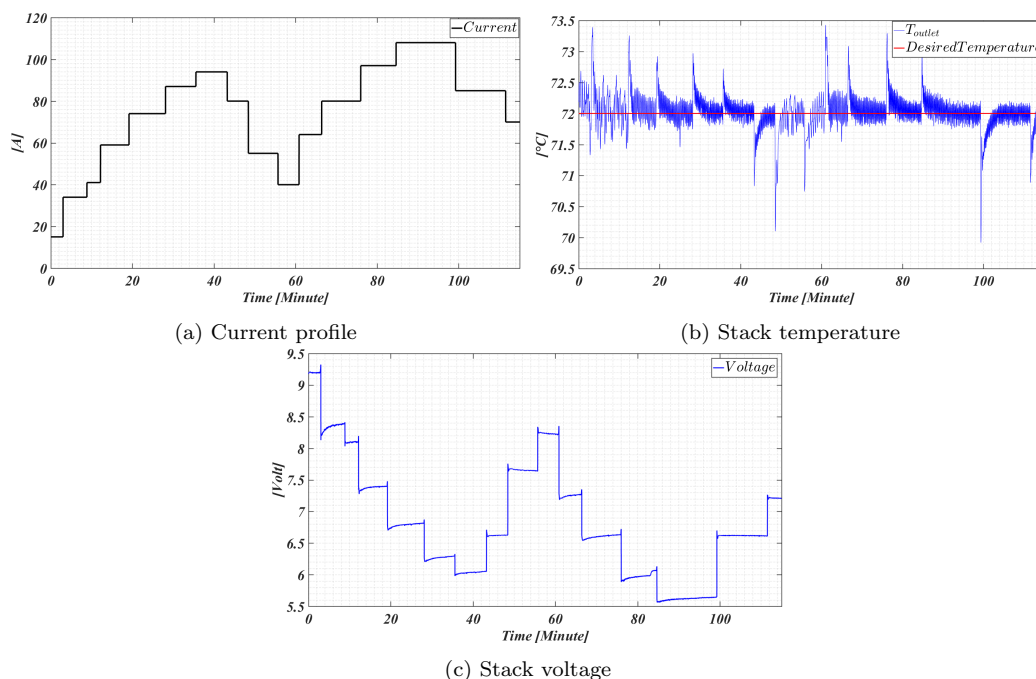
(c) Stack voltage

Figure 4: Stack temperature control

The two experimental tests presented in this section have two objectives: firstly, ensuring that the PEM fuel cell operates under favorable operating conditions with the proposed control strategy. Secondly, it is necessary to point out that a smooth temperature control is insufficient in the event of a fault on the stack temperature sensor. The consequences of such a fault on the operation of the fuel cell are discussed in the following section.

5. Water management diagnosis

The proposed strategy for detecting water management faults is focused on the estimation of the cathode inlet pressure. As explained in the previous section, the inlet gas pressure is controlled to maintain a low pressure at the stack inlet. Accordingly, the cathode inlet pressure cannot increase since it is always controlled to remain

20

at the desired value throughout the presence of excess water in the cells. However, when water condensation occurs, the estimated inlet cathode pressure deviates. The effect of water condensation fault is considered as a disturbance for the controller and as a fault for the diagnosis approach. The residual signal used for the detection of water condensation in the cells is given by Eq.33.

Nevertheless, an estimation of the outlet stack temperature is also performed. The intention is to detect a fault in the stack temperature management. The fault is simulated by introducing an offset on the value provided by the sensor. The normal temperature operation condition is 72 °C. A change in the desired temperature is made to determine the parameter β_{temp} for this operating point. Fig.5 shows the estimated and measured outlet temperature in fault free case. It is necessary to remember that the parameter β_{temp} used for the correction of the estimated outlet temperature is recomputed at at each change of setpoint or current. In the transient state, $y_{Tout}(t) = \beta_{temp}\hat{y}_{Tout}(t)$ since $\beta_{temp}(t)$ evolves and is not constant, which does not allow the detection of sensor fault in the transient states [4min - 11min] and [23min - 34min].
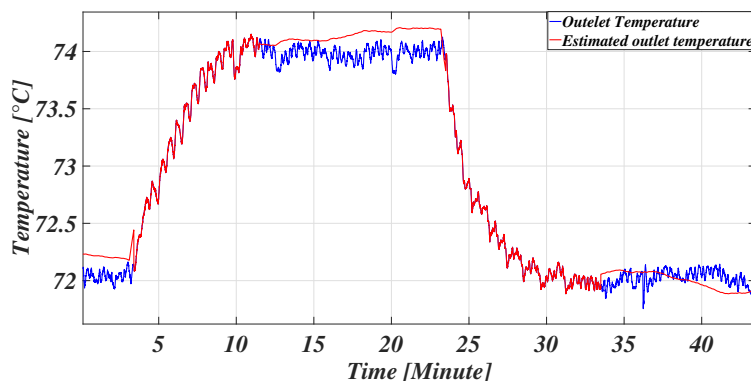

Figure 5: Estimated and outlet stack temperature

5.1. Water condensation in the cells

The stack operating conditions are: temperature $72°C$, cooling rate $1l/min$, air and hydrogen stoichiometry 2. The temperature sensor fault is triggered as follows:

$$y_{Tout}(t) = T_{out}(t) + f \tag{41}$$

Where T_{out} refers to the real temperature of the stack and y_{Tout} is the measured one. f refers the offset related to the amplitude of the fault on the sensor. In case of $f = 0$ no fault exists, i.e. $y_{All} = T_{All}$. Whereas for $f \neq 0$ the fault on the sensor

is generated, $y_{Tout} \neq T_{out}$. For this experimental part, the fault is simulated with $f = 27°C$.

The residual signal is calculated as follows:

$$r_{temperature}(t) = y_{Tout}(t) - \beta_{temp}\hat{y}_{Tout}(t) \tag{42}$$

One of the objectives of the proposed method is to maintain the inlet pressure difference at 0bar. This purpose is ensured for all the test as shown in Fig.6(a). At the beginning of the test, the inlet pressure is established at 1400 mbar. An increase of 400 mbar is applied to improve PEMFC performance and to determine the value of β_p for the studied operating point as seen in Fig.7(a). This increase is reflected in the voltage signal which rises as illustrated in Fig.6(c). The overall time of the experience is 70 min, from the beginning of the test until 22nd minute a normal operating condition is considered. From [23 min to 45 min] the temperature sensor fault is present. From 45th minute to the end of the test the fault is removed, i.e $f = 0$.

Under normal operating condition the estimated outlet temperature fits clearly with the measured, as shown in Fig.6(b). Once the sensor fault is present at 23rd minute, the considered temperature for the controller is 89°C, which is referred to the faulty outlet temperature in Fig.6(b). Therefore, the controller reacts by cooling the PEM fuel cell until the faulty outlet temperature stabilizes at 72°C. The residual signal diverges from 0 directly at the moment of a sensor fault occurrences, which facilitates fault detection, see Fig.6(d).

Once a sensor fault occurs, the controller corrects the error between the desired and the measured temperature caused by a fault. However, in reality, this correction action leads to the cooling of the stack, which results in the change of the operating conditions that provokes the PEMF voltage drop as illustrated in Fig.6(c).

(a) Inlet pressure difference

(b) Estimated, real and measured temperature

(c) Stack voltage
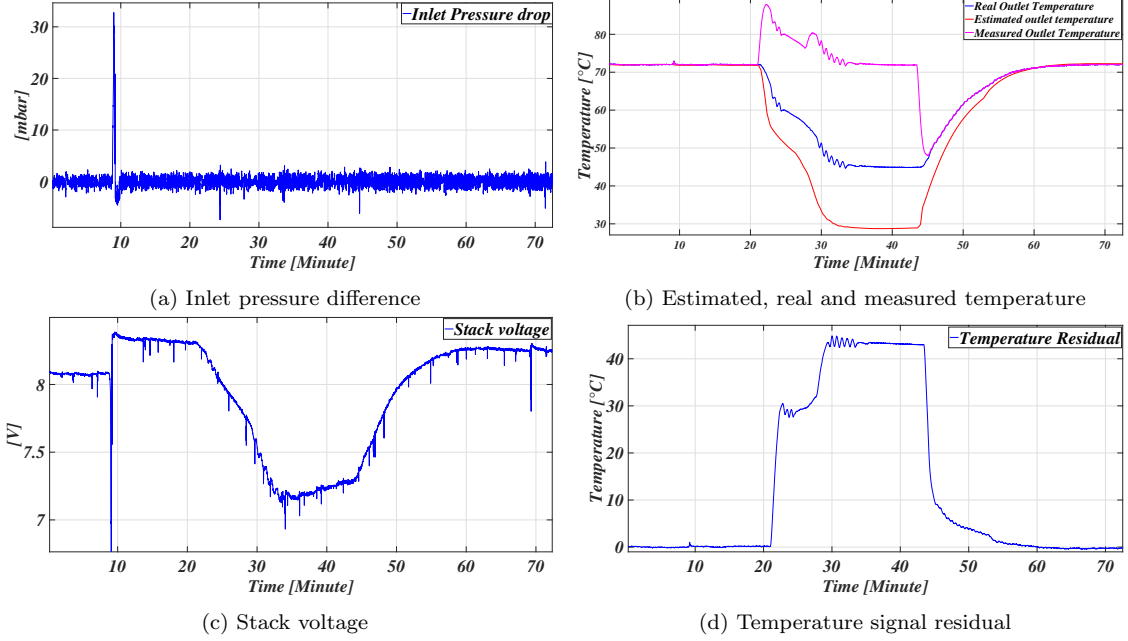
(d) Temperature signal residual

Figure 6: Sensor fault detection

The estimated inlet cathode pressure corresponds to the measured one up to the 31st minute a divergence starts to occur as seen in Fig.7(a,(b)). This might be related to the fact that water starts to accumulate in the cells.

The residual signal is noisy as shown in Fig.7(d). In order to reduce false detection, the residual analysis is performed with the Cumulative sum with an sliding window CUSUM [60]. The following procedure is employed to calculate the residual CUSUM:

- Computation of the mean $m_{rp}(0)$ for the initial residual samples r_p.

- Initialize the $cusum_{rp}(1) = r_p(1) - m_{rp}(0)$.

- Calculate $m_{rp}(t)$ of $r_p(t)$ over a moving interval $[t - N, t]$, where N is the length of the moving interval.

- $cusum_{rp}(t) = cusum_{rp}(t - 1) + r_p(t) - m_{rp}(t)$.

The CUSUM residual signal confirms this discrepancy and exceeds the threshold at the 32nd minute as shown in Fig.7(e). Once the residual cusum exceeds the threshold, a fault in water management is detected, in particular the fault of water condensation in the cells. The determination of the threshold is performed in an empirical way and according to the normal operation conditions. To confirm that

23

the proposed method allows the water condensation detection, a cathodic pressure drop signal is illustrated in Fig.7(c). It is observed that the cathode pressure drop increases with residue evolution, which confirms the presence of an excess of water in the stack. Temperature sensor fault is cancelled at the 45th minute, which means that the controller considers the actual stack temperature which is 45°C. Due to the disappearance of the fault, the outlet estimated temperature of the stack starts to follow the measured temperature until the 60th minute, the two signals overlap, Fig.6(b). The cusum residual signal returns below the threshold at the 48th minute. This indicates that the water content of cells is presently relatively stable. Once the temperature is stabilized at its initial value, the residual used for sensor fault detection returns to 0 at the 60th minute and stay around this value until the end of the test as shown in Fig.6(d).

Water condensation inside the stack has been detected at an early stage. Then it reduces the time when the stack is exposed to flooding and avoids a severe flooding which could lead to starvation fault.

5.2. Drying fault detection

The operating conditions for this experiment are the same as for the previous one. The whole experience lasts 43 minutes. In contrast with the previous case, the sensor fault is introduced by a negative value $f = -8$°C. Similarly, the inlet pressure is controlled to maintain the same magnitude for each setpoint change. The PEM fuel cell operates at 1700mbar, a change of set point is made at the 7min to reach this desired set point as seen in Fig.9(a). Stack inlet pressure drop is kept near 0 Bar throughout the test, as illustrated Fig.8(a). The estimated outlet temperature follows the measured one until the sensor fault occurs at the 12nd minute, Fig.8(b). The faulty outlet temperature is the temperature used by the controller to regulate the PEM fuel cell temperature. For this reason, the real stack temperature evolves up to 80°C as shown in Fig.8(b). The temperature residual differs from 0 as soon as the sensor fault occurs as seen in Fig.8(c). The stack voltage starts to drop at the 15th minute.
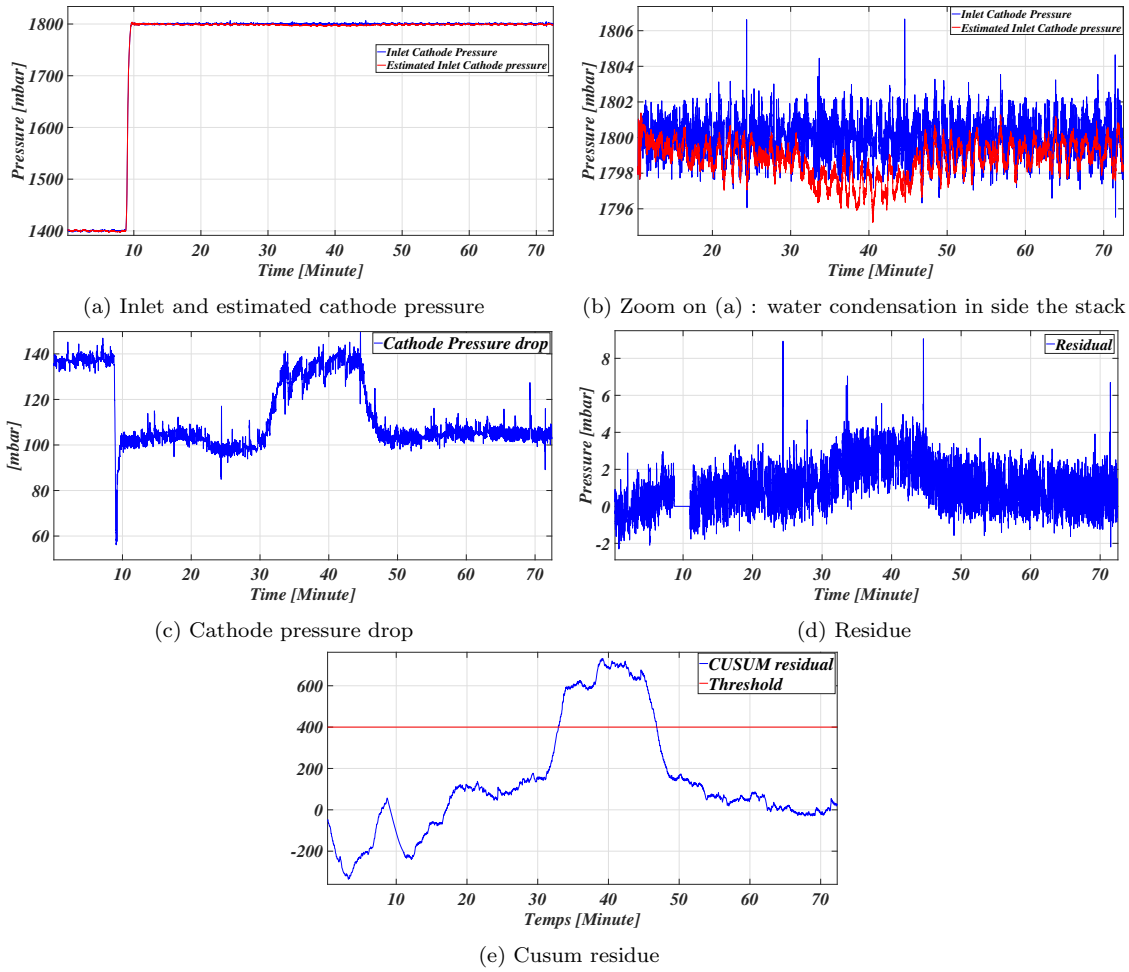
(a) Inlet and estimated cathode pressure

(b) Zoom on (a) : water condensation in side the stack

(c) Cathode pressure drop

(d) Residue

(e) Cusum residue

Figure 7: Detection of water condensation in the stack

(a) Inlet pressure difference

(b) Estimated, real and measured temperature
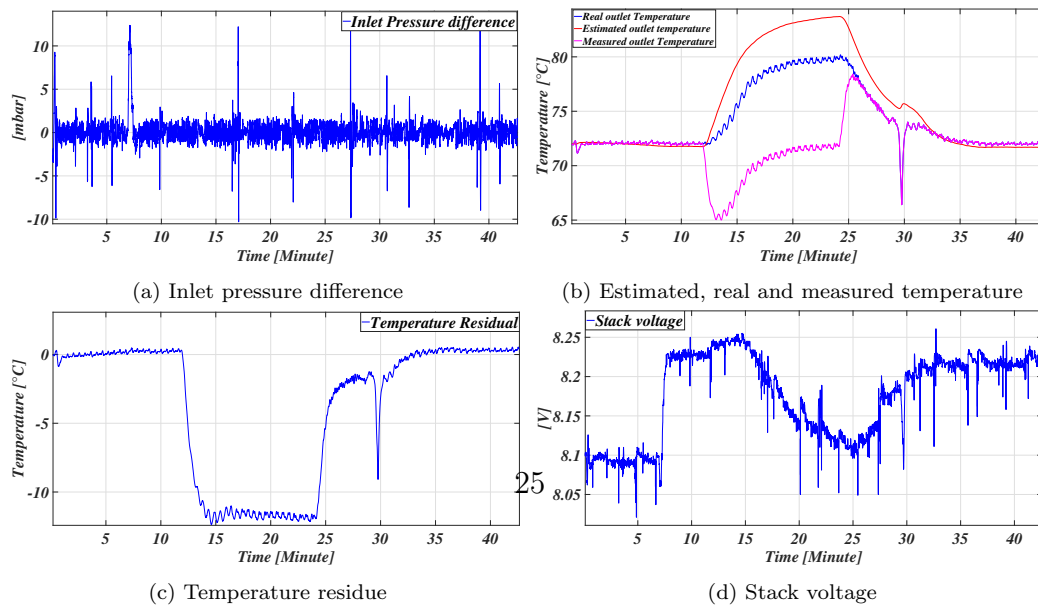
(c) Temperature residue

(d) Stack voltage

Figure 8: Sensor fault detection : membrane dehydration

25

The estimated inlet pressure follows the measured pressure and there is no discrepancies noted throughout the test, Fig.9(a,b), since the drying fault has no impact on the cathode side pressure. The cathodic pressure drop remains constant also for the entire length of the test as shown in Fig.9(c). The residual fault indicator used for the estimation of the cathode inlet pressure remains around 0, even when the drying fault occurs, as illustrated in Fig.9(d).

The sensor fault is removed at the 25th minute. This results in the convergence of the estimated output temperature to the real one up to the 35th minute, as shown Fig.8(b). Even the voltage signal returns to its initial value, which means that the membrane has re-hydrated once the operating conditions have been restored.

(a) Inlet and estimated cathode pressure

(b) zoom on (a)

(c) Cathode pressure drop

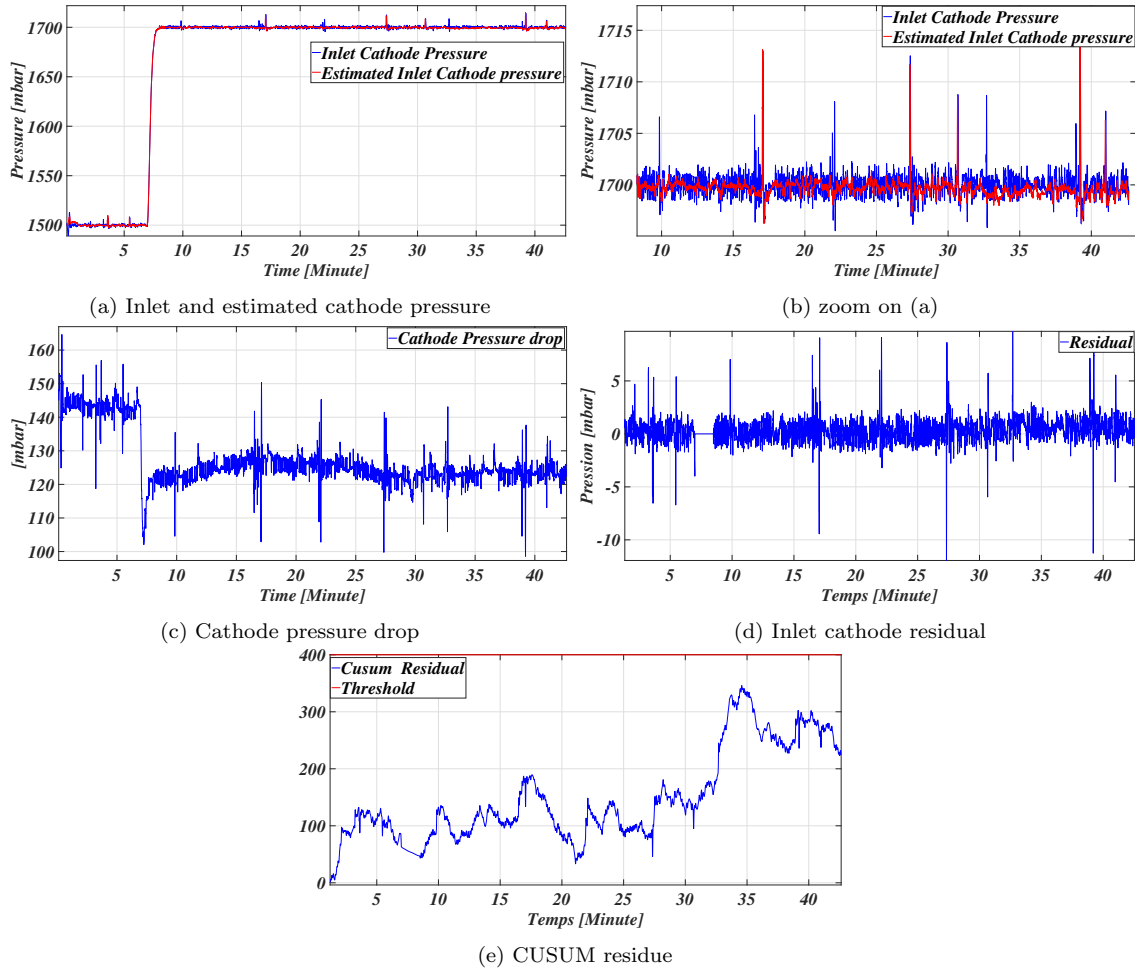(d) Inlet cathode residual

(e) CUSUM residue

Figure 9: Membrane dehydration fault

The stack voltage drop is a symptom of fault presence. To detect and isolate faults related to water management, two residuals are generated. In the case of water condensation in the cells, the fault is detected and isolated by the change of the two residues. For membrane dehydration case, only the temperature residual and the voltage drop occur.

6. Discussion

PEM fuel cell diagnosis is addressed in this paper by establishing a link between a control of the stack operating conditions and fault detection. The literature presents a wide variety of methods used for diagnosing the water management of PEMFC. Mostly, theses faults are generated by the voluntary change of PEMFC operating conditions such as temperature [47] [45] [41][46] [48], relative humidity [45] [44] [40] [43] and gas stoichiometry [42][46]. The control of these operating conditions is usually ignored in their studies. Indeed, with a robust controller to disturbances and system parametric uncertainties, these operating conditions are maintained at the desired operating conditions. This is verified unless there is a fault that impacts the actuator and/or the sensor of a control loop. Depending on the severity of the fault, this can affect the controllability and observability of the system.
For this purpose, first, it is proposed, to control the stack temperature and inlet pressure with model-free controller to ensure smooth stack operation. Secondly, a new diagnosis approach that is inspired by model-free control is presented and applied to PEMFC diagnosis. The developed method is employed to detect a fault in stack temperature which results in faults related to water management that is also detected.
In the overall view of the PEMFC diagnosis, in the present study, the water management faults are studied as a consequence of the temperature sensor fault. This fault is detected in real time at the instant of its manifestation without any requirement of the PEMFC analytical model. Unlike [61] authors use the accurate model of the temperature management system to detect and isolate the sensor fault. Authors in [62] use a data driven classification method coupled with deep learning algorithm, which is not based on the PEMFC model. The approach requires a significant quantity of data with offline training, which makes real-time application challenging task. In related work, the impact of temperature management faults on PEMFC operation is not considered.
Concerning water management fault diagnosis, in the case of water condensation, the fault is detected after 10 minutes of the occurrence of a sensor fault. This detection time is considered satisfactory for limiting severe PEMFC degradation.

27

Membrane dehydration and water condensation in the cells fault are detected without any requirement of additional sensors. Even measuring the outlet cathode pressure is unnecessary in the proposed strategy, which limits the number of additional sensors. It is interesting to highlight that the proposed method offers the opportunity to both control the operating conditions of the PEMFC and detect potential faults that may affect it. Such a double performance is not provided by the already existing PEMFC diagnosis methods. These advantages and the way of addressing the diagnosis of fuel cell water management are making the proposed approach a novelty compared to the existing methods in the literature.

However, this method presents a limitation for fault detection in the transient regime for highly nonlinear systems as PEMFC. This is mainly due to the β parameter used for the correction of the estimated output which requires a readjustment. Consequently, in this study, all the considered faults are detected in steady state.

7. Conclusion

In the present paper, water management fault diagnosis is treated as the result of a sensor stack temperature fault. A novel diagnosis approach in a model-free context is presented and validated in real time on a 1.2 kW fuel cell. The overall conclusion can be synthesized as follows:

1. In order to ensure the PEMFC proper operation, the control of stack temperature and inlet pressure are ensured with model-free control. The applied controller is based on an ultra-local model that is continuously updated, absolutely not on the precise model of the PEMFC.

2. A theoretical proof is presented for model-free fault detection. The developed diagnosis method is mainly relied on the estimation of the ultra-local model output that is used in the control part. Any deviation of the calculated residue is considered as an indication of fault presence. Firstly, the proposed diagnosis method is applied to detect a loss of back pressure performance. This fault is studied to illustrate the proposed method as an initiation to water management diagnosis.

3. The fault in temperature sensor is the principal cause of water condensation in the cells and membrane dehydration. All theses faults are detected and isolated in real time by evaluating the residuals of stack temperature and cathode inlet pressure.

4. The proposed approach does not rely on precise knowledge of the model and offers the possibility to control the system and detect a fault. However, the model-free fault detection requires some improvements to be able to detect

faults in transient conditions. This is mainly due to the necessity to recalculate the β parameter used in the residual generation.

Nomenclature

α	Controller design parameter
$\hat{y}$	Estimated system output
$\hat{y}_{inO2}$	Estimated inlet air pressure
$\hat{y}_{Tout}$	Estiamted outlet temperature
f	Sensor fault
r_p	Residual of the cathode side
$r_{temperature}$	Temperature residual
$Tout$	Real outlet stack temperature
y	Measured system output
y_{Cool}	Measured cooling flow rate
y_{inH2}	Measured inlet hydrogen pressure
y_{inO2}	Measeured inlet air pressure
y_{Tin}	Measured inlet stack temperature
y_{Tout}	Measured outlet stack temperature

References

[1] M. A. Mohammed, I. A. Mohammed, R. A. Hasan, N. Ţăpuş, A. H. Ali, O. A. Hammood, Green energy sources: issues and challenges, in: 2019 18th RoEduNet Conference: Networking in Education and Research (RoEduNet), IEEE, 2019, pp. 1–8.

[2] T. Choudhary, et al., Computational analysis of ir-sofc: thermodynamic, electrochemical process and flow configuration dependency, international journal of hydrogen energy 41 (2016) 1259–1271.

[3] K. Scott, A. Shukla, Polymer electrolyte membrane fuel cells: Principles and advances, Reviews in Environmental Science and Bio/Technology 3 (2004) 273–280.

[4] T. Choudhary, et al., Thermodynamic assessment of advanced sofc-blade cooled gas turbine hybrid cycle, International Journal of Hydrogen Energy 42 (2017) 10248–10263.

[5] P. Costamagna, S. Srinivasan, Quantum jumps in the pemfc science and technology from the 1960s to the year 2000: Part ii. engineering, technology development and application aspects, Journal of power sources 102 (2001) 253–269.

[6] T. Choudhary, et al., Computational analysis of ir-sofc: Transient, thermal stress, carbon deposition and flow dependency, International journal of hydrogen energy 41 (2016) 10212–10227.

[7] W. Schmittinger, A. Vahidi, A review of the main parameters influencing long-term performance and durability of pem fuel cells, Journal of power sources 180 (2008) 1–14.

[8] N. Yousfi-Steiner, P. Moçotéguy, D. Candusso, D. Hissel, A. Hernandez, A. Aslanides, A review on pem voltage degradation associated with water management: Impacts, influent factors and characterization, Journal of power sources 183 (2008) 260–274.

[9] S. Kim, I. Hong, Effects of humidity and temperature on a proton exchange membrane fuel cell (pemfc) stack, Journal of Industrial and Engineering Chemistry 14 (2008) 357–364.

[10] P. Pei, H. Chen, Main factors affecting the lifetime of proton exchange membrane fuel cells in vehicle applications: A review, Applied Energy 125 (2014) 60–75.

[11] H. Askaripour, Effect of operating conditions on the performance of a pem fuel cell, International Journal of Heat and Mass Transfer 144 (2019) 118705.

[12] R. Petrone, Z. Zheng, D. Hissel, M.-C. Péra, C. Pianese, M. Sorrentino, M. Becherif, N. Yousfi-Steiner, A review on model-based diagnosis methodologies for pemfcs, International Journal of Hydrogen Energy 38 (2013) 7077–7091.

[13] M. Ait Ziane, M. Pera, C. Join, M. Benne, J. Chabriat, N. Y. Steiner, C. Damour, On-line implementation of model free controller for oxygen stoichiometry and pressure difference control of polymer electrolyte fuel cell, International Journal of Hydrogen Energy (2022).

[14] A. M. Ali, C. Join, F. Hamelin, Fault diagnosis without a priori model, Systems & control letters 61 (2012) 316–321.

[15] R. Isermann, An introduction from fault detection to fault tolerance, 2006.

[16] P. M. Frank, Fault diagnosis in dynamic systems using analytical and knowledge-based redundancy: A survey and some new results, automatica 26 (1990) 459–474.

[17] W. Li, H. Li, S. Gu, T. Chen, Process fault diagnosis with model-and knowledge-based approaches: Advances and opportunities, Control Engineering Practice 105 (2020) 104637.

[18] T. Wang, L. Liang, S. K. Gurumurthy, F. Ponci, A. Monti, Z. Yang, R. W. De Doncker, Model-based fault detection and isolation in dc microgrids using optimal observers, IEEE Journal of Emerging and Selected Topics in Power Electronics 9 (2020) 5613–5630.

[19] S. Rahme, N. Meskin, Adaptive sliding mode observer for sensor fault diagnosis of an industrial gas turbine, Control Engineering Practice 38 (2015) 57–74.

[20] C. Join, H. Sira-Ramírez, M. Fliess, Control of an uncertain three-tank system via on-line parameter identification and fault detection, IFAC Proceedings Volumes 38 (2005) 251–256.

[21] Z. Shi, X. Yang, Y. Li, G. Yu, Wavelet-based synchroextracting transform: An effective tfa tool for machinery fault diagnosis, Control Engineering Practice 114 (2021) 104884.

[22] Z. Gao, C. Cecati, S. X. Ding, A survey of fault diagnosis and fault-tolerant techniques—part i: Fault diagnosis with model-based and signal-based approaches, IEEE transactions on industrial electronics 62 (2015) 3757–3767.

[23] Y. Zhao, S. Wang, F. Xiao, A statistical fault detection and diagnosis method for centrifugal chillers based on exponentially-weighted moving average control charts and support vector regression, Applied Thermal Engineering 51 (2013) 560–572.

[24] R. Liu, B. Yang, E. Zio, X. Chen, Artificial intelligence for fault diagnosis of rotating machinery: A review, Mechanical Systems and Signal Processing 108 (2018) 33–47.

[25] E. Garoudja, A. Chouder, K. Kara, S. Silvestre, An enhanced machine learning based approach for failures detection and diagnosis of pv systems, Energy conversion and management 151 (2017) 496–513.

[26] R. Isermann, Fault-diagnosis systems: an introduction from fault detection to fault tolerance, Springer Science & Business Media, 2005.

[27] M. Fliess, C. Join, Model-free control, International Journal of Control 86 (2013) 2228–2252.

[28] J. Hu, L. Xu, J. Li, C. Fang, S. Cheng, M. Ouyang, P. Hong, Model-based estimation of liquid saturation in cathode gas diffusion layer and current density difference under proton exchange membrane fuel cell flooding, international journal of hydrogen energy 40 (2015) 14187–14201.

[29] X. Zhang, P. Pisu, An unscented kalman filter based on-line diagnostic approach for pem fuel cell flooding, International Journal of Prognostics and Health Management 5 (2014).

[30] I. H. Kazmi, A. I. Bhatti, Parameter estimation of proton exchange membrane fuel cell system using sliding mode observer, International Journal of Innovative Computing, Information and Control 8 (2012) 5137–5148.

[31] D. Shin, S. Yoo, Y.-H. Lee, On-line water contents diagnosis of pemfc based on measurements, International Journal of Precision Engineering and Manufacturing-Green Technology 7 (2020) 1085–1093.

[32] J. Wu, X. Z. Yuan, H. Wang, M. Blanco, J. J. Martin, J. Zhang, Diagnostic tools in pem fuel cell research: Part ii: Physical/chemical methods, International Journal of Hydrogen Energy 33 (2008) 1747–1757.

[33] K. Jiao, B. Zhou, P. Quan, Liquid water transport in parallel serpentine channels with manifolds on cathode side of a pem fuel cell stack, Journal of Power Sources 154 (2006) 124–137.

[34] W. He, G. Lin, T. Van Nguyen, Diagnostic tool to detect electrode flooding in proton-exchange-membrane fuel cells, AIChE Journal 49 (2003) 3221–3228.

[35] Y. Li, P. Pei, Z. Wu, P. Ren, X. Jia, D. Chen, S. Huang, Approaches to avoid flooding in association with pressure drop in proton exchange membrane fuel cells, Applied energy 224 (2018) 42–51.

[36] H. Ma, H. Zhang, J. Hu, Y. Cai, B. Yi, Diagnostic tool to detect liquid water removal in the cathode channels of proton exchange membrane fuel cells, Journal of Power Sources 162 (2006) 469–473.

[37] S.-S. Hsieh, Y.-J. Huang, Measurements of current and water distribution for a micro-pem fuel cell with different flow fields, Journal of Power Sources 183 (2008) 193–204.

[38] P. Pei, Y. Li, H. Xu, Z. Wu, A review on water fault diagnosis of pemfc associated with the pressure drop, Applied Energy 173 (2016) 366–385.

[39] M. Song, P. Pei, H. Zha, H. Xu, Water management of proton exchange membrane fuel cell based on control of hydrogen pressure drop, Journal of Power Sources 267 (2014) 655–663.

[40] N. Y. Steiner, D. Hissel, P. Moçotéguy, D. Candusso, Diagnosis of polymer electrolyte fuel cells failure modes (flooding & drying out) by neural networks modeling, International journal of hydrogen energy 36 (2011) 3067–3075.

[41] E. Pahon, D. Hissel, S. Jemei, N. Y. Steiner, Signal-based diagnostic approach to enhance fuel cell durability, Journal of Power Sources 506 (2021) 230223.

[42] E. Pahon, N. Y. Steiner, S. Jemei, D. Hissel, P. Moçoteguy, A signal-based method for fast pemfc diagnosis, Applied Energy 165 (2016) 748–758.

[43] A. H. Detti, S. Jemei, S. Morando, N. Y. Steiner, Classification based method using fast fourier transform (fft) and total harmonic distortion (thd) dedicated to proton exchange membrane fuel cell (pemfc) diagnosis, in: 2017 IEEE Vehicle Power and Propulsion Conference (VPPC), IEEE, 2017, pp. 1–6.

[44] A. Dib, R. Maizia, S. Martemianov, A. Thomas, Statistical short time analysis for proton exchange membrane fuel cell diagnostic-application to water management, Fuel Cells 19 (2019) 539–549.

[45] S. Zhou, Y. Lu, D. Bao, K. Wang, J. Shan, Z. Hou, Real-time data-driven fault diagnosis of proton exchange membrane fuel cell system based on binary encoding convolutional neural network, International Journal of Hydrogen Energy 47 (2022) 10976–10989.

[46] Y. Ao, S. Laghrouche, D. Depernet, Diagnosis of proton exchange membrane fuel cell system based on adaptive neural fuzzy inference system and electrochemical impedance spectroscopy, Energy Conversion and Management 256 (2022) 115391.

[47] C. Damour, M. Benne, B. Grondin-Perez, M. Bessafi, D. Hissel, J.-P. Chabriat, Polymer electrolyte membrane fuel cell fault diagnosis based on empirical mode decomposition, Journal of Power Sources 299 (2015) 596–603.

[48] S. Jiang, Q. Li, R. Gan, W. Chen, Fault diagnosis for pemfc water management subsystem based on learning vector quantization neural network and kernel principal component analysis, World Electric Vehicle Journal 12 (2021) 255.

[49] N. Yousfi-Steiner, P. Moçotéguy, D. Candusso, D. Hissel, A. Hernandez, A. Aslanides, A review on pem voltage degradation associated with water management: Impacts, influent factors and characterization, Journal of power sources 183 (2008) 260–274.

[50] M. Ait Ziane, C. Join, M.-C. Pera, N. Y. Steiner, M. Benne, C. Damour, A new method for fault detection in a free model context, IFAC-PapersOnLine 55 (2022) 55–60.

[51] M. Ait Ziane, N. Y. Steiner, C. Join, M. Benne, C. Damour, M. C. Péra, Model-free fault detection: application to polymer electrolyte fuel cell system, in: 2022 10th International Conference on Systems and Control (ICSC), IEEE, 2022, pp. 340–345.

[52] M. Fliess, Model-free control and intelligent pid controllers: towards a possible trivialization of nonlinear control?, IFAC Proceedings Volumes 42 (2009) 1531–1550.

[53] L. Menhour, B. d'Andréa Novel, M. Fliess, D. Gruyer, H. Mounier, An efficient model-free setting for longitudinal and lateral vehicle control: Validation through the interconnected pro-sivic/rtmaps prototyping platform, IEEE Transactions on Intelligent Transportation Systems 19 (2017) 461–475.

[54] J. M. Barth, J.-P. Condomines, M. Bronz, J.-M. Moschetta, C. Join, M. Fliess, Model-free control algorithms for micro air vehicles with transitioning flight capabilities, International Journal of Micro Air Vehicles 12 (2020) 1756829320914264.

[55] M. Fliess, H. Sira-Ramirez, Closed-loop parametric identification for continuous-time linear systems via new algebraic techniques, in: Identification of Continuous-time Models from sampled Data, Springer, 2008, pp. 363–391.

[56] M. Mboup, C. Join, M. Fliess, Numerical differentiation with annihilators in noisy environment, Numerical algorithms 50 (2009) 439–467.

[57] M. Mboup, Parameter estimation for signals described by differential equations, Applicable Analysis 88 (2009) 29–52.

[58] M. Haddar, R. Chaari, S. C. Baslamisli, F. Chaari, M. Haddar, Intelligent pd controller design for active suspension system based on robust model-free control strategy, Proceedings of the Institution of Mechanical Engineers, Part C: Journal of Mechanical Engineering Science 233 (2019) 4863–4880.

[59] J. M. Olszanecki Barth, J.-P. Condomines, M. Bronz, G. Hattenberger, J.-M. Moschetta, C. Join, M. Fliess, Towards a unified model-free control architecture for tailsitter micro air vehicles: Flight simulation analysis and experimental flights, in: AIAA Scitech 2020 Forum, 2020, p. 2075.

[60] O. A. Grigg, V. Farewell, D. Spiegelhalter, Use of risk-adjusted cusum and rsprtcharts for monitoring in medical contexts, Statistical methods in medical research 12 (2003) 147–170.

[61] C. Yan, J. Chen, H. Liu, H. Lu, Model-based fault tolerant control for the thermal management of pemfc systems, IEEE Transactions on Industrial Electronics 67 (2019) 2875–2884.

[62] B. Zuo, Z. Zhang, J. Cheng, W. Huo, Z. Zhong, M. Wang, Data-driven flooding fault diagnosis method for proton-exchange membrane fuel cells using deep learning technologies, Energy Conversion and Management 251 (2022) 115004.